



## Constraints on mantle flow at the Caribbean–South American plate boundary inferred from shear wave splitting

Mark A. Growdon,<sup>1</sup> Gary L. Pavlis,<sup>1</sup> Fenglin Niu,<sup>2</sup> Frank L. Vernon,<sup>3</sup> and Herbert Rendon<sup>4</sup>

Received 20 June 2008; revised 7 October 2008; accepted 12 November 2008; published 7 February 2009.

[1] We measured shear wave splitting from *SKS* and *SKKS* data recorded by temporary stations deployed as part of the Broadband Onshore-Offshore Lithospheric Investigation of Venezuela and the Antilles Arc Region project and the national seismic network of Venezuela. Approximately 3000 station-event pairs yielded ~300 with visible *SKS* and/or *SKKS* phases. We obtained 63 measurements at 39 of the 82 stations in the network using the method of Silver and Chan (1991) and conventional quality criteria. We combined our results with previous measurements made by Russo et al. (1996). The most prominent feature in the data is an area of large (>2.0 s) lag times with roughly east–west fast axes in northeastern Venezuela. Mineral physics models show split times this large are difficult to explain with horizontal foliation, but are more feasible with anisotropy characterized by a coherent vertical foliation and an east–west fast axis extending over most of the upper 250 km of the mantle. We interpret the large split times in northeastern Venezuela as a consequence of eastward translation of the Atlantic slab, which has left a strong vertical foliation in its wake parallel to the plate boundary. The peak split times correspond closely with the point the slab intersects the base of the anisotropic asthenosphere at 250 km. Away from this area of large split times the measured times fall to more standard values, but an east–west fast axis still predominates. We suggest this is linked to the rapidly varying strain field at the southern edge of the Atlantic which quickly disrupts the coherent strain field that causes the very large split times in northeastern Venezuela.

**Citation:** Growdon, M. A., G. L. Pavlis, F. Niu, F. L. Vernon, and H. Rendon (2009), Constraints on mantle flow at the Caribbean–South American plate boundary inferred from shear wave splitting, *J. Geophys. Res.*, 114, B02303, doi:10.1029/2008JB005887.

### 1. Introduction

[2] Estimating upper mantle flow direction is a first-order problem in understanding plate tectonics. The geometry of mantle flow at plate boundaries in general, and in corner regions in particular, are poorly understood. One method to approach this problem is to measure the shear wave splitting of *SKS* or *SKKS* phases to infer anisotropic fabric in the upper mantle [e.g., Silver and Chan, 1991; Fouch and Rondenay, 2006]. This correlation of mantle flow and seismic anisotropy has been established through observations of natural samples, seismic properties coupled with experimental studies, and theoretical models [e.g., Fouch and Rondenay, 2006; Savage, 1999; Silver, 1996]. This paper makes an assumption that shear wave splitting measurements are created by lattice-preferred orientations that we can link to mantle flow through directions of inferred

anisotropy. In this paper we present new measurements of shear wave splitting in the boundary region between the Caribbean (Ca) and South American (SA) plates (Figure 1) that provide new constraints on mantle flow in this tectonic corner.

[3] Russo et al. [1996] conducted the first shear wave splitting study in the southeast Caribbean region. They found unusually large split times in comparison to other South American plate measurements [Silver, 1996]. The new measurements presented here utilize a recent set of data collected as part of the Broadband Onshore-Offshore Lithospheric Investigation of Venezuela and the Antilles Arc Region (BOLIVAR) project [Levander et al., 2006]. The BOLIVAR project deployed stations in the same region studied by Russo et al. [1996] but extending over a much larger portion of the plate boundary (Figure 1). We combine the BOLIVAR data with measurements from Russo et al. [1996] to test several working hypotheses that have been posed to explain Caribbean tectonics: (1) Caribbean underthrusting of SA [Pindell et al., 1988], (2) independent motion of the Maracaibo block [Audemard and Audemard, 2002], and (3) Lesser Antilles Arc subduction as either a hinge geometry [Govers and Wortel, 2005; Molnar and Sykes, 1969] or tensile tear geometry [Clark et al., 2008; VanDecar et al., 2003]. In

<sup>1</sup>Department of Geological Sciences, Indiana University, Bloomington, Indiana, USA.

<sup>2</sup>Department of Earth Science, Rice University, Houston, Texas, USA.

<sup>3</sup>Scripps Institution of Oceanography, University of California, San Diego, La Jolla, California, USA.

<sup>4</sup>FUNVISIS, Caracas, Venezuela.

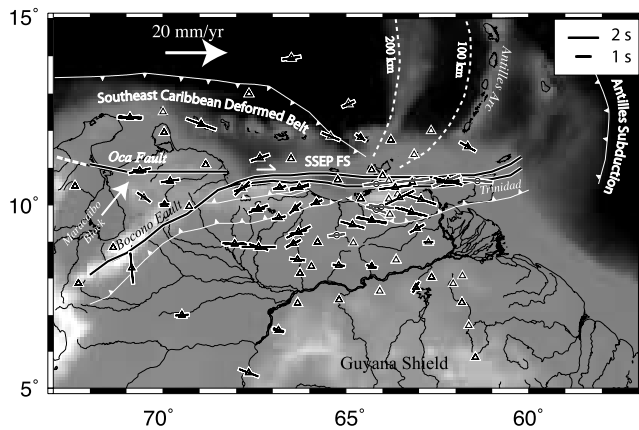


**Figure 1.** *S* wave splitting results for southeast Caribbean region. Base map is bathymetry/topography scaled by elevation with black as the lowest elevation. Seismic stations analyzed in this study are shown as triangles, and stations analyzed by *Russo et al.* [1996] are shown as circles. *S* wave splitting measurements are shown as conventional line segments drawn through station symbol. The line is oriented in the measured fast axis direction with a length proportional to the measured split time. The time scale is displayed at the top right corner. Results from this study are drawn with black symbols, while results from *Russo et al.* [1996] are drawn with gray symbols. Symbols with no lines are stations that yielded no acceptable *S* wave splitting measurements. Base map shows major tectonic features for the region. Black lines are major strike-slip faults, and white lines are thrust systems with the teeth pointed downdip. The SSEP FS label refers to the San Sebastian–El Pilar Fault System, a major strike-slip system commonly viewed as the plate boundary between South America and the Caribbean. The dashed lines labeled 100 km and 200 km are contours of depth to the top of the subducting Atlantic slab estimated from seismicity by *Miller et al.* [2009]. Large arrows show approximate plate motions relative to South America of the Caribbean and the Maracaibo Block.

addition, these data provide some of the first measurements that can be used to investigate whether mantle flow changes as the setting changes from a subduction and transpressional zone [*Weber et al.*, 2001] into a stable craton with a possible continental keel mantle geometry.

## 2. Tectonic Setting

[4] The BOLIVAR array (Figure 1) was deployed over one of the most complicated tectonic settings on Earth. The focus of the experiment was the Ca-SA plate boundary. The Ca plate is moving  $\sim 20$  mm/a eastward relative to the SA plate [e.g., *Pérez et al.*, 2001; *Weber et al.*, 2001]. In the crust, this motion is taken up by the El Pilar–San Sebastian dextral strike slip zone (Figure 1) [e.g., *Levander et al.*, 2006; *Audemard and Audemard*, 2002]. We stress that Figure 1 illustrates the El Pilar–San Sebastian system as a nearly linear feature, but the actual deformation takes place in a broad zone within the east–west mountain belt in northern Venezuela bounded on the south by the thrust systems illustrated in Figure 1. It has been suggested that the eastern boundary of the Caribbean plate slab is inducing a rollback of

the Antilles arc linked to flow around the subduction systems in western South American [*Russo and Silver*, 1994]. The Antilles volcanic arc is a surficial marker of Atlantic subduction (Figure 1). Two first-order features of the Antilles arc that are important for this paper are as follows: (1) the volcanic arc terminates directly north of Trinidad, and (2) deep earthquakes linked to subduction terminate around the latitude of Trinidad. This basic observation led *Molnar and Sykes* [1969] to postulate that this plate margin was formed by a shear tear with the currently active tear in the crust near Trinidad. More recently, *Clark et al.* [2008] examined the shearing tear hypothesis and a competing hypothesis of an extensional tear in light of recent active source seismic results from the BOLIVAR project. They concluded that the shear tear, or hinge geometry, best fits the new seismic data. This paper presents additional evidence that supports this hypothesis.

[5] The E-W trending, dextral, El Pilar–San Sebastian system extends westward from Trinidad until it bifurcates into the Bocono fault system and Oca fault systems near  $68^\circ$  west (Figure 1). The Bocono fault system trends  $\sim N45E$  and extends through the Venezuelan Andes defining the eastern side of the Maracaibo Block [*Audemard and Audemard*, 2002]. The Maracaibo Block, one of several hypothesized micro blocks in this region, is being extruded NE at  $\sim 10$  mm/a relative to SA plate along the Bocono fault [*Pérez et al.*, 2001; *Audemard and Audemard*, 2002]. The Maracaibo Block and the Venezuelan Andes are covered by the western stations of the BOLIVAR array. The northern edge of the Maracaibo Block is cut by the Oca fault, a dextral strike-slip fault system oriented approximately east–west that merges with the El Pilar–San Sebastian system.

[6] The Maracaibo and western Venezuela regions are most likely influenced by the paleo-Ca and Nazca plates' subductions dipping east beneath the Maracaibo block and northwest SA, respectively [*Van der Hilst and Mann*, 1994; *Taboada et al.*, 2000; *Bosch*, 1997; *Bezada et al.*, 2008]. The geometry of subduction in this tectonic corner is far from clear. The paleo-Ca plate in particular may be influencing mantle dynamics below the Maracaibo Block with the northern slab edge trending along the east–west Oca fault. This creates a similar geometry under the Maracaibo Block as the Atlantic subduction creates beneath eastern Venezuela, but details of the geometry are poorly constrained.

## 3. Data

[7] The BOLIVAR array is a composite of 82 broadband, digital stations assembled from several sources. The core of the array is the recently installed national network of Venezuela operated by the Fundación Venezolana de Investigaciones Sismológicas (FUNVISIS). The FUNVISIS network consists of 34 digital broadband stations sampled at 100 samples per second. The permanent stations were extended with three temporary broadband instrument deployments: (1) 27 Program for Array Seismic Studies of the Continental Lithosphere (PASSCAL) stations operated from November 2003 to May 2005, (2) 13 ocean bottom seismometers (OBS) operated from February 2004 to February 2005, and (3) a Rice University deployment of 8 seismic stations operated from November 2004 to November 2005

[Niu *et al.*, 2007]. Both the PASSCAL and Rice stations were sampled at 40 samples per second, while the OBS instruments used a sample rate of 31.25 samples per second. We used estimates of sensor orientation from Niu *et al.* [2007] to align the OBS data.

[8] We visually examined *SKS* and *SKKS* phases for all events with magnitudes of 6.0 or larger chosen within a range of  $80^\circ$  to  $140^\circ$ . Of the original  $\sim 3000$  *SKS* and *SKKS* event-station pairs identified,  $\sim 10\%$  were found to have a visible signal.

#### 4. Data Analysis

[9] Silver and Chan [1991] describe two possible methods for making shear wave splitting measurements from *SKS* and *SKKS* phases: the particle linearization method (PLM) and the transverse energy minimization method (TEM). Our study takes an approach similar to that of Fouch *et al.* [2000] by first making the measurement with the PLM method and verifying the results with TEM method results. Both measurement methods require choices with regard to several critical issues: windowing about the phase to be measured, uncertainty analysis calculation, and selection criteria to specify what constitutes a reliable measurement.

[10] This shear wave splitting method requires a window to be chosen around the phase to be measured. The choice of window width is arbitrary and varies widely in the literature, but there is general agreement that the window must be equal to or greater than 10 s due to the dominant period of *SKS* and *SKKS* phases seen in real data [Wolfe and Silver, 1998]. Windows as large as 40 s are used (M. J. Fouch, personal communications, 2007). All measurements presented here have passed a windowing robustness test conducted as follows: (1) we chose a window on the order of 10 to 20 s duration spanning the main *SKS* or *SKKS* pulse, and (2) we varied the bounds on either side of this basic window by several seconds. We rejected measurements that were heavily dependent on the window position.

[11] Silver and Chan [1991] describe methods to estimate the uncertainty of shear wave splitting measurement for both the TEM and PLM methods. In both cases the uncertainty calculation assumes that the corrected transverse component is representative of the instantaneous background noise. The residual energy on the transverse component is used to calculate the number of degrees of freedom, which reduces to a scaling factor for the uncertainty estimate. Because uncertainty measurements are often debated, we chose to supplement the Silver and Chan uncertainty measurements with the more conservative method introduced by Yang *et al.* [1995]. The main difference is that Yang *et al.* [1995] calculate the number of degrees of freedom from preevent noise. We note, however, that because of significant long-period noise on most of the BOLIVAR stations we were forced to filter the noise segments with a 2–15 s period filter. We justify this filter by noting that the average windowing size is 15 s, so noise of periods longer than the window should minimally affect the measurement. Without this restriction we found that the autocorrelation of preevent noise, which is the basis of the Yang *et al.* [1995] method, provided an overly pessimistic error estimate because of the red spectrum of the noise field.

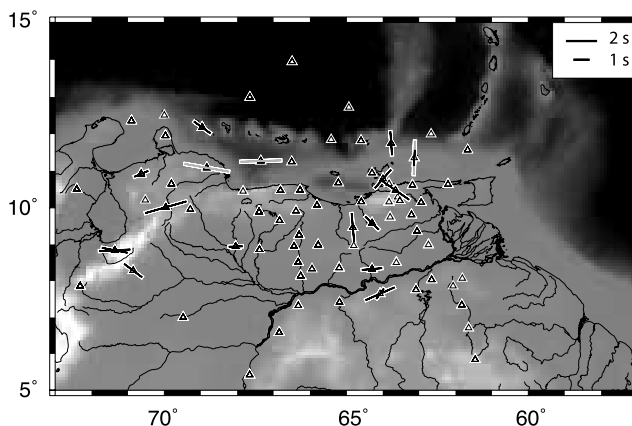


**Figure 2.** Rejected *S* wave splitting measurements. Symbols and base map are as described in Figure 1, but we have omitted tectonic features for clarity. *S* wave splitting measurements rejected for inconsistency of PLM and TEM estimates are drawn with black symbols. Measurements reported by Growdon [2007] but rejected on later review due to low signal to noise are plotted with gray symbols.

[12] For consistency we used a fixed set of criteria to establish which measurements could be ranked as reliable. Measurements were accepted only if the following criteria were satisfied: (1) particle motion is roughly elliptical before correction and linear in shape afterward, (2) the uncertainty plot shows a well defined minimum, (3) the fast polarization direction is not parallel or perpendicular to the back azimuth direction for that event within the estimated 95% confidence interval, (4) windowing is robust (see above), and (5) the TEM method solution verifies the PLM measurements within the estimated 95% confidence intervals. The fifth criterion is becoming more common [e.g., Fouch *et al.*, 2000; Polet and Kanamori, 2002]. We suggest that this criterion may be particularly useful for weeding out measurements that acquire erroneous split times due to complex slab and mantle flow geometries that are likely in this region. These geometries can create reflections or multiples that could corrupt this measurement technique. Because this criterion is not universally applied, Figure 2 shows all measurements that satisfied the first four criteria along with those rejected by criteria 5. We would argue that Figure 2 shows the measurements rejected by this criteria are generally inconsistent with more robust measurements made at these same stations and with nearby stations. Thus, we would argue using this added windowing criteria is prudent for these data.

[13] Figure 2 also shows three additional measurements that we have removed from our summary results for a different reason. These three measurements were included in plots by Growdon [2007], but tertiary review of the measurements led us to conclude all were unreliable. There were two primary reasons for this conclusion. First, the particle motion linearity criteria of our rule set is somewhat subjective and all three were marginal measurements in this regard. Second, signal to noise can be a difficult thing to properly characterize in secondary phases like *SKS* and *SKKS*. When we viewed the seismograms for these three measurements in a broader context (all BOLIVAR stations from the same event viewed with a longer time window) we

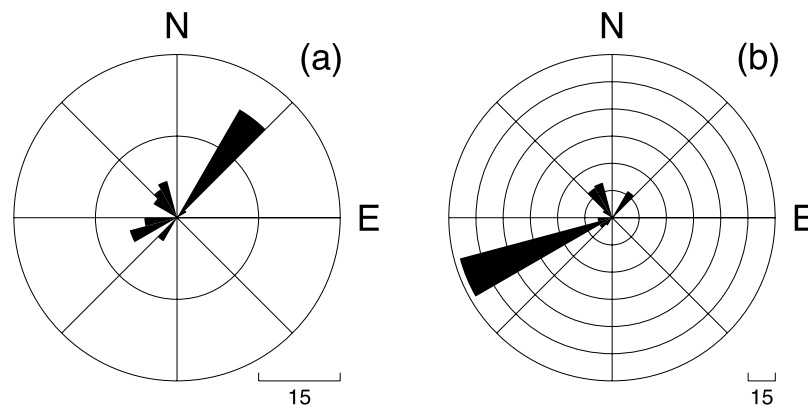


**Figure 3.** Event azimuth distribution. (a) A rose diagram of counts of all measurements plotted in Figure 1. Azimuth direction of a great circle path from an array center located in Caracas, Venezuela, to each source (back azimuth). (b) A similar diagram for data rejected due because the source back azimuth was within the error bounds of the estimated fast axis. Both plots have circles plotted at radii scaled to multiples of counts of 15. Note that the range in Figure 3b is much larger than Figure 3a illustrating the large fraction of data rejected by this criteria.

judged the signal-to-noise ratio to be insufficient to make the measurements reliable.

[14] We conclude this section by emphasizing that although the winnowing criteria we used are conventional, they are quite conservative. As a result,  $\sim 300$  feasible seismograms only yielded 66 reliable measurements on 43 of the 82 stations. A second reason why so few measurements survived this winnowing is clarified by Figure 3. As noted in the earlier study by *Russo et al.* [1996] the most active source area for *SKS* data in this region is the southwest Pacific, but the back azimuth for events from that region is westerly. Since the predominant fast direction revealed in the reliable measurements is east–west, a large fraction of the measurements failed the null direction test (criteria 3 above). *Wolfe and Silver* [1998] suggest their multiple event averaging method can utilize null measurements effectively, but experiments we did including all the null measurements in this method did not yield more stable results. We suspect the reason is that the null data outnumber the reliable data in this case. We considered criteria for including only “good” null measurements, but found no objective way to judge “good.” Hence, we include only single stations measurements of splitting parameters in this paper and present this as a challenge to others to expand this data set with other measurement techniques. For comprehensive figures showing graphics of all the measurements the reader is referred to *Growdon* [2007].

## 5. Interpretation

[15] The first observation the reader should understand is that the shear wave split times observed here are all consistently quite large. The times observed are consistently in the range of 1.5 to 2.5 s (Figure 1 and Tables S1 and S2 in the auxiliary material).<sup>1</sup> Normal crustal split times are on the order of 0.3–0.4 s. Oceanic lithosphere and stable craton

areas usually exhibit shear wave splitting times on the order of 0.5–1.5 s and the mean global split time is 1.0 s [*Silver*, 1996]. Split times larger than  $\sim 0.5$  s are generally considered to require significant mantle anisotropy [e.g., *Savage*, 1999]. *Savage* [1999] points out that split times greater than 2.0 s cannot, in general, be explained with anisotropy confined to the upper mantle above 220–250 km. However, the current viewpoint seems to be that anisotropic fabric formation below a 220–250 km depth is difficult to maintain with normal mantle geotherms. While there is some evidence for anisotropy below this depth it is most likely a small contribution to the total [e.g., *Conrad et al.*, 2007; *Fouch and Rondenay*, 2006; *Padilha et al.*, 2006; *Savage*, 1999; *Vinnik et al.*, 1992]. Since we have several measurements with split times larger than 2.0 s, if we accept *Savage*’s assertion, then something unusual is required to explain these observations.

[16] The “something unusual” that we suggest is the cause of these large split times is illustrated in Figure 4. It has been recognized since *Molnar and Sykes* [1969] that the mantle beneath northeastern Venezuela and Trinidad contains the southern limit of the subducting Atlantic. *Molnar and Sykes* [1969] were also the first to hypothesize that the geometry here is an unusual hinge fault geometry with the Atlantic essentially tearing like a piece of paper. *Clark et al.* [2008] provides the most recent refinement of this model by combining the results of onshore-offshore refraction experiments and receiver function results from the BOLIVAR array [*Niu et al.*, 2007]. The basic geometry of the Atlantic slab terminating along the northern boundary of South America is reasonably well established from numerous lines of evidence. Furthermore, the prevailing model of the dominant tectonic environment of the northern boundary of South America for the past 30 Ma is the progressive propagation of this tectonic corner from a point at least as far west as the bifurcation point of the El Pilar–San Sebastian system into the Bocono and Oca Faults (Figure 1) to the present location near Trinidad [e.g., *Pindell et al.*, 1988]. The main new insight the shear wave splitting results add to this model is that we claim these data are consistent with a nearly pure rollback of the Atlantic relative to South

<sup>1</sup>Auxiliary materials are available in the HTML. doi:10.1029/2008JB005887.

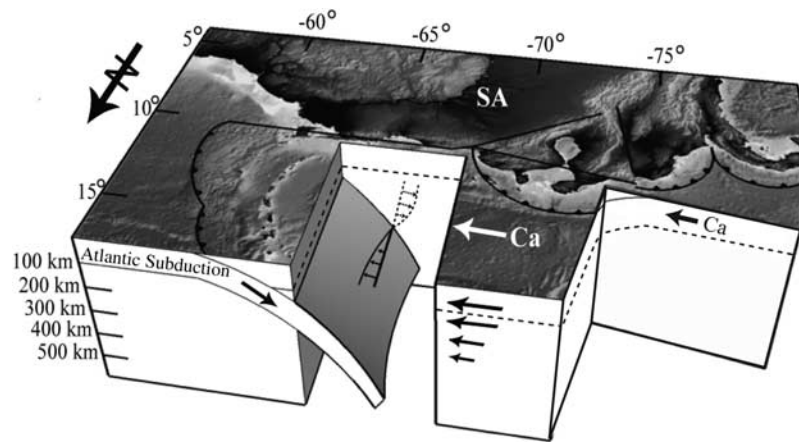


**Figure 4.** Three-dimensional block diagram of a model for the southeast Caribbean plate boundary. The surface image is a Mercator projection of digital topography with sketched structural faults modeled after *Taboada et al.* [2000] and *Levander et al.* [2006]. The approximate geometry of the Caribbean and South American plates is illustrated. The dashed lines on all edges show a 100 km depth horizon on this scaled diagram. Arrows in the area above the Atlantic slab show the direction of flow in the upper mantle that we argue is necessary to explain the shear wave splitting results. That is, the data imply shearing parallel to the plate boundary as illustrated. Similar arrows are sketched under the Caribbean illustrating our interpretation of the implied flow field.

America with a flow regime dominated by the geometry illustrated in Figure 4. The key feature illustrated there is the idea that the eastward motion of the southern edge of the Atlantic slab relative to South America has induced a vertically oriented shear zone in its wake. We claim this shear zone is the source of the very high shear wave splitting times seen in northeastern Venezuela. To support this claim, we need to review the current views on how shear wave splitting relates to mantle flow processes.

[17] The prevailing model used to explain *SKS* splitting measurements is anisotropy induced by preferred orientation of olivine and pyroxene in the upper mantle. Lattice preferred orientation as a mechanism for producing seismic anisotropy is widely held to be constrained to the mantle shallower than 250 km where dislocation glide mechanisms control the deformation. [e.g., *Conrad et al.*, 2007; *Fouch and Rondenay*, 2006; *Padilha et al.*, 2006; *Savage*, 1999; *Vinnik et al.*, 1992]. The bottom of the anisotropic region of the mantle is controlled by temperature. At deeper depths Coble and/or Nabarro-Herring creep processes begin to dominate to produce a more isotropic rock fabric. Although there are ongoing debates on how laboratory data relate to samples collected from nature, the prevailing view today is that two different deformation modes can produce the same orientation of the fast axis [see, e.g., *Tikoff et al.*, 2004, Figure 1]. The implication of the petrologic/mineral physics results for the southeast Caribbean is that east–west fast axes can be explained one of two different ways: (1) simple shear in the asthenosphere from an east–west absolute plate motion (horizontal foliation with the fast axis of olivine aligned in an east–west direction), or (2) a vertical shear zone in the asthenosphere (vertical foliation with the fast axis of olivine horizontal and oriented in an east–west direction). Although these are normally two radically different deformation modes (the maximum shear plane orientations are 90° apart) the three-dimensional model illustrated in Figure 4 shows a way

this can be reconciled. We suggest these data can be explained by assuming the anisotropy under the Caribbean plate is dominated by east–west translation of the Caribbean over the deeper mantle. This would induce simple shear under the lithosphere that could produce a horizontal foliation and an associated east–west fast axis for the anisotropy in the upper 250 km of the mantle. In contrast, we suggest that this fabric must terminate at the northern boundary of South America. The *S* wave splitting data and the basic geometry suggest the shear strain must transition into a vertical shear zone parallel to the El Pilar fault system and the associated plate boundary. As suggested earlier by others [*Russo et al.*, 1996; *Tikoff et al.*, 2004] we can expect a vertical shear zone along the plate boundary. Vertical foliation of the mantle with an east–west fast axis is consistent with the relative plate motion across this boundary.

[18] Although previous workers [*Russo et al.*, 1996] have recognized the fact that a vertical shear zone is most consistent with splitting observations along the plate boundary in Venezuela, until this paper no one seems to have emphasized the primary agent of this deformation mode: the eastward motion of the slab edge relative to South America. As the Antilles arc translated from west to east, the passing slab would impart a strong vertical foliation on the asthenosphere at its southern edge. The strongest foliation would be expected to occur directly above the point where the subducting slab intersects the base of the anisotropic portion of the mantle (nominally 200 to 250 km). In addition to this simple geometric argument the subduction process can also be expected to depress the temperature at the southern edge of the Atlantic slab thus potentially lowering the transition depth from anisotropic to isotropic fabric. With time (equivalent to distance west in this model) the fabric would likely weaken as the boundary transitioned to a broader shear zone required by the eastward motion of the Caribbean relative to South America. Figure 1 shows

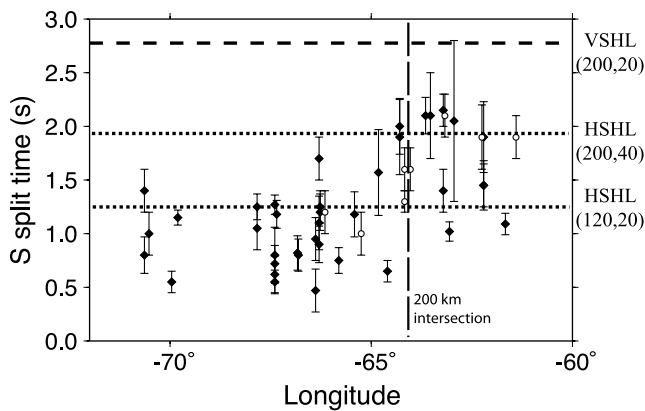


**Figure 5.** *S* wave splitting magnitude along the Caribbean–South American plate boundary. We plot the measured *S* wave splitting magnitudes from this study and *Russo et al.* [1996] as a function of longitude. To clarify the strong peak in splitting magnitude near longitude 63.5°, we plot only data for stations between latitudes of 9° and 12°. For reference the vertical dashed line is the approximate intersection of the 200 km subduction contour with the San Sebastian–El Pilar system illustrated in Figure 1. Error bars were computed as described in the text. Horizontal dashed lines refer to predictions from mineral physics models discussed in the text.

that in this region this is exactly the pattern we see. Figure 5 is a more quantitative demonstration of the same. It shows that the largest split times occur between 63° and 64° west longitude, which Figure 1 shows correlates with the intersection of the 200 km contour of the top Atlantic slab. The Atlantic lithosphere has a finite thickness so this area links directly to the point where the base of the Atlantic lithosphere intersects the predicted base of the anisotropic region of the asthenosphere.

[19] Figure 5 also provides more quantitative evidence that the large split times seen in eastern Venezuela are linked to a vertical foliation of the asthenosphere. We applied results of a numerical model by *Estey and Douglas* [1986] to predict the magnitude of *S* wave splitting. Their paper is useful as it predicts split times for both vertical foliation and horizontal foliation using standard models of mantle lithology. Later papers [e.g., *Tommasi et al.*, 2000; *Blackman and Kendall*, 2002; *Tikoff et al.*, 2004] show similar results, but *Estey and Douglas* [1986] is particularly useful for this paper because it contains graphical results that an interested reader can readily evaluate themselves. Figure 5 shows three predictions of *S* wave split times from *Estey and Douglas* [1986]. At the lower end the line at 1.3 s is the prediction for horizontal foliation with a 100 km thick anisotropic region (20 km thick “cap” described in their paper). An intermediate value is an upper bound of just under 2 s predicted for a 200 km thick (40 km cap) anisotropic layer. Finally, the largest split time is predicted for mantle with a vertical foliation and the same thickness (200 km with a 20 km cap) as the upper bound value for horizontal foliation (2 s line in Figure 5). Vertical foliation produces larger splitting than comparable thicknesses of horizontally foliated rock because their model allows for an orthorhombic symmetry. In the vertical folia-

tion case the direction of wave propagation relative to the symmetry axes is orthogonal to that of the more conventional horizontal case.

[20] The predictions from *Estey and Douglas* [1986] are important for our interpretation in two ways. The first is that the size of the split times predicted for a material with a horizontal foliation compared to a vertical foliation is different. Although a horizontal foliation is feasible (a 2 s split time is within the error bars of all the measurements seen in Figure 5), a very thick (200 km) vertically coherent layer is required to produce split times that large. This general result from mineral physics was used earlier by *Russo et al.* [1996] to argue for a vertically oriented fabric in this same area and we concur with their interpretation.

[21] The second prediction from mineral physics is that *Estey and Douglas* [1986] and many other later papers demonstrate that splitting magnitudes vary through one of two different means. Either the thickness of the anisotropic layer with a coherent fabric can vary or the direction of foliation can be rotated. In this location we suspect these are alternative but hardly mutually exclusive explanations for these data. In the latter case, these and similar models show that rotating the foliation direction from horizontal to vertical while keeping the fast axis direction fixed can increase the split times by up to 40%. A rotation of the fabric away from one of the two end-members (horizontal or vertical foliation) can be inferred by variations in splitting magnitude with event azimuth [e.g., *Schulte-Pelkum and Blackman*, 2003]. Unfortunately, the number of measurements we were able to make from these data are completely inadequate to make such an interpretation. The most measurements we obtained for any station was 5 (Table S1 of the auxiliary material). We suggest that the very large variation in split times seen in this area are caused by the superposition of variations in thickness and orientation of upper mantle fabric. We would argue that the peak splitting magnitudes over 2 s are associated with the thickest region of mantle with a coherent fabric. The geometry suggests strongly that a coherent vertical shear zone would be a reasonable model from the Moho to the depth where dislocation climb processes break down the anisotropic fabric. This is normally between 200 and 250 km depth, but we reiterate that the subducting Atlantic is likely to cool the mantle in this region which could potentially further thicken the anisotropic region with a completely coherent fabric. Away from this peak the splitting magnitudes are probably reduced by rotation of the fabric out of the vertical plane. We suggest this is most likely a 90° rotation of the foliation northward into the central Caribbean where the fabric is probably better explained as a horizontal foliation with an east–west fast axis. What actually happens under South America is more ambiguous as the data are more irregular and the plate geometry nearly demands it be more variable. For instance, *Russo and Silver* [1994] argue that the upper mantle flow field in this area is impacted by flow around the edges of the entire South American subduction system. These data are consistent with that model if the overall Caribbean motion is viewed as a fragment of the lithosphere caught in this larger-scale process. That larger-scale flow process, however, is likely further modulated by thickened lithosphere [*Landes and Pavlis*, 2008] under the Guyana shield.

Thus, there is every reason to suspect the flow field under all of Venezuela varies rapidly in all three dimensions causing a highly variable upper mantle fabric. The results shown in Figure 1 are consistent with this larger-scale model.

[22] **Acknowledgments.** Multiple agencies are gratefully acknowledged that made the data for this work possible. These include FUNVISIS; the IRIS-PASSCAL facility of the National Science Foundation; the Ocean Bottom Seismic Instrument Pool facility at the University of California, San Diego; and Rice University. The BOLIVAR project was supported by NSF-Continental Dynamics Program award EAR0338487, EAR0607580, EAR0003544, EAR0607685, and EAR022270. M.G. acknowledges support from Chevron Corp. for a fellowship that supported part of his graduate studies. The paper benefited greatly from constructive comments by Martha Savage and an anonymous reviewer.

## References

- Audemard, F. E., and F. A. Audemard (2002), Structure of the Merida Andes, Venezuela: Relations with the South America-Caribbean geodynamic interaction, *Tectonophysics*, *345*, 299–327, doi:10.1016/S0040-1951(01)00218-9.
- Bezada, M. J., M. Schmitz, M. I. Jacome, J. Rodriguez, F. Audemard, C. Izarra, and the BOLIVAR Active Seismic Working Group (2008), Crustal structure in the Falcón Basin area, northwestern Venezuela, from seismic and gravimetric evidence, *J. Geodyn.*, *45*, 191–200, doi:10.1016/j.jog.2007.11.002.
- Blackman, D. K., and J.-M. Kendall (2002), Seismic anisotropy in the upper mantle: 2. Predictions for current plate boundary flow models, *Geochem. Geophys. Geosyst.*, *3*(9), 8602, doi:10.1029/2001GC000247.
- Bosch, M. (1997), P wave velocity tomography of the Venezuelan region from local arrival times, *J. Geophys. Res.*, *102*, 5455–5472, doi:10.1029/96JB03172.
- Clark, S. A., M. Sobiesiak, C. A. Zelt, M. B. Magnani, M. S. Miller, M. J. Bezada, and A. Levander (2008), Identification and tectonic implications of a tear in the South American plate at the southern end of the Lesser Antilles, *Geochem. Geophys. Geosyst.*, *9*, Q11004, doi:10.1029/2008GC002084.
- Conrad, C. P., M. D. Behn, and P. G. Silver (2007), Global mantle flow and the development of seismic anisotropy: Differences between the oceanic and continental upper mantle, *J. Geophys. Res.*, *112*, B07317, doi:10.1029/2006JB004608.
- Estey, L. H., and B. J. Douglas (1986), Upper mantle anisotropy: A preliminary model, *J. Geophys. Res.*, *91*, 11,393–11,406.
- Fouch, M. J., and S. Rondenay (2006), Seismic anisotropy beneath stable continental interiors, *Phys. Earth Planet. Inter.*, *158*, 292–320, doi:10.1016/j.pepi.2006.03.024.
- Fouch, M. J., K. M. Fischer, E. M. Parmentier, M. E. Wyssession, and T. J. Clarke (2000), Shear wave splitting, continental keels, and patterns of mantle flow, *J. Geophys. Res.*, *105*, 6255–6275, doi:10.1029/1999JB900372.
- Govers, R., and M. J. R. Wortel (2005), Lithosphere tearing at STEP faults: Response to edges of subduction zones, *Earth Planet. Sci. Lett.*, *236*, 505–523, doi:10.1016/j.epsl.2005.03.022.
- Growdon, M. A. (2007), Interpretation of shear wave splitting measurements at the Caribbean-South American plate boundary, M.S. thesis, 42 pp., Indiana Univ., Bloomington.
- Landes, M., and G. L. Pavlis (2008), New constraints on the Caribbean-South America plate boundary from S wave receiver functions, *Eos Trans. AGU*, *89*(53), Fall Meet. Suppl., Abstract T53B-1924.
- Levander, A., F. Niu, T. A. C.-Lee, and X. Cheng (2006), Imag (in)ing the continental lithosphere, *Tectonophysics*, *416*, 167–185, doi:10.1016/j.tecto.2005.11.018.
- Miller, M. S., A. Levander, F. Niu, and A. Li (2009), Upper mantle structure beneath the Caribbean-South American plate boundary from surface wave tomography, *J. Geophys. Res.*, *114*, B01312, doi:10.1029/2007JB005507.
- Molnar, P., and L. R. Sykes (1969), Tectonics of the Caribbean and Middle America regions from focal mechanisms and seismicity, *Geol. Soc. Am. Bull.*, *80*, 1639–1684, doi:10.1130/0016-7606(1969)80[1639:TOTCAM]2.0.CO;2.
- Niu, F., T. Bravo, G. Pavlis, F. Vernon, H. Rendon, M. Bezada, and A. Levander (2007), Receiver function study of the crustal structure of the southeastern Caribbean plate boundary and Venezuela, *J. Geophys. Res.*, *112*, B11308, doi:10.1029/2006JB004802.
- Padilha, A. L., et al. (2006), Lithospheric and sublithospheric anisotropy beneath central-southeastern Brazil constrained by long-period magnetotelluric data, *Phys. Earth Planet. Inter.*, *158*, 190–209, doi:10.1016/j.pepi.2006.05.006.
- Pérez, O. J., R. Bilham, R. Bendick, J. R. Velandia, N. Hernández, C. Moncayo, M. Hoyer, and M. Kozuch (2001), Velocity field across the southern Caribbean plate boundary and estimates of Caribbean-South American plate motion using GPS geodesy 1994–2000, *Geophys. Res. Lett.*, *28*, 2987–2990, doi:10.1029/2001GL013183.
- Pindell, J. L., et al. (1988), A plate-kinematic framework for models of Caribbean evolution, *Tectonophysics*, *155*, 121–138, doi:10.1016/0040-1951(88)90262-4.
- Polet, J., and H. Kanamori (2002), Anisotropy beneath California: Shear wave splitting measurements using a dense broadband array, *Geophys. J. Int.*, *149*, 313–327, doi:10.1046/j.1365-246X.2002.01630.x.
- Russo, R. M., and P. G. Silver (1994), Trench-parallel flow beneath the Nazca plate from seismic anisotropy, *Science*, *263*, 1105–1111, doi:10.1126/science.263.5150.1105.
- Russo, R. M., et al. (1996), Shear-wave splitting in northeast Venezuela, Trinidad, and the eastern Caribbean, *Phys. Earth Planet. Inter.*, *95*, 251–275, doi:10.1016/0031-9201(95)03128-6.
- Savage, M. K. (1999), Seismic anisotropy and mantle deformation: What have we learned from shear wave splitting?, *Rev. Geophys.*, *37*, 65–106, doi:10.1029/98RG02075.
- Schulte-Pelkum, V., and D. K. Blackman (2003), A synthesis of seismic P and S anisotropy, *Geophys. J. Int.*, *154*, 166–178, doi:10.1046/j.1365-246X.2003.01951.x.
- Silver, P. G. (1996), Seismic anisotropy beneath the continents: Probing the depths of geology, *Annu. Rev. Earth Planet. Sci.*, *24*, 385–432, doi:10.1146/annurev.earth.24.1.385.
- Silver, P. G., and W. W. Chan (1991), Shear-wave splitting and subcontinental mantle deformation, *J. Geophys. Res.*, *96*, 16,429–16,454, doi:10.1029/91JB00899.
- Taboada, A., L. A. Rivera, A. Fuenzalida, A. Cisternas, H. Philip, H. Bijwaard, J. Olaya, and C. Rivera (2000), Geodynamics of the northern Andes: Subductions and intracontinental deformation (Colombia), *Tectonics*, *19*, 787–813, doi:10.1029/2000TC900004.
- Tikoff, B., R. Russo, C. Teyssier, and A. Tommasi (2004), Mantle-driven deformation of orogenic zones and clutch tectonics, in *Vertical Coupling and Decoupling in the Lithosphere*, edited by J. Grocott et al., *Geol. Soc. Spec. Publ.*, *227*, 41–64.
- Tommasi, A., D. Mainprice, G. Canova, and Y. Chastel (2000), Viscoplastic self-consistent and equilibrium-based modeling of olivine lattice preferred orientations: Implications for the upper mantle seismic anisotropy, *J. Geophys. Res.*, *105*, 7893–7908, doi:10.1029/1999JB900411.
- VanDecar, J. C., R. M. Russo, D. E. James, W. B. Ambeh, and M. Franke (2003), A seismic continuation of the Lesser Antilles slab beneath continental South America, *J. Geophys. Res.*, *108*(B1), 2043, doi:10.1029/2001JB000884.
- van der Hilst, R., and P. Mann (1994), Tectonic implications of tomographic images of subducted lithosphere beneath northwestern South America, *Geology*, *22*, 451–454, doi:10.1130/0091-7613(1994)022<0451:TIOTIO>2.3.CO;2.
- Vinnik, L. P., et al. (1992), Global patterns of azimuthal anisotropy and deformations in the continental mantle, *Geophys. J. Int.*, *111*, 433–447, doi:10.1111/j.1365-246X.1992.tb02102.x.
- Weber, J. C., et al. (2001), GPS estimate of relative motion between the Caribbean and South American plates, and geologic implications for Trinidad and Venezuela, *Geology*, *29*, 75–78, doi:10.1130/0091-7613(2001)029<0075:GEORMB>2.0.CO;2.
- Wolfe, C. J., and P. G. Silver (1998), Seismic anisotropy of oceanic upper mantle: Shear wave splitting methodologies and observations, *J. Geophys. Res.*, *103*, 749–771, doi:10.1029/97JB02023.
- Yang, X. P., et al. (1995), Seismic anisotropy beneath the Shumagin Islands segment of the Aleutian-Alaska subduction zone, *J. Geophys. Res.*, *100*, 18,165–18,177, doi:10.1029/95JB01425.

M. A. Growdon and G. L. Pavlis, Department of Geological Sciences, Indiana University, 1001 East 10th Street, Bloomington, IN 47405, USA. (markgrowdon@gmail.com; pavlis@indiana.edu)

F. Niu, Department of Earth Science, Rice University, 6100 Main Street, Houston, TX 77005, USA.

H. Rendon, Departamento Ciencias de la Tierra, Prolongacion Calle Mara, Urbanizacion El Llanito, Apartado Postal 76880, 1070 Caracas, Venezuela.

F. L. Vernon, Scripps Institution of Oceanography, University of California, San Diego, 9500 Gilman Drive, La Jolla, CA 92093, USA.